The effect of the association of near infrared laser therapy, bone morphogenetic proteins, and guided bone regeneration on tibial fractures treated with internal rigid fixation: A Raman spectroscopic study

Cibele B. Lopes,[1] Marcos T. T. Pacheco,[2] Landulfo Silveira, Jr.,[2] Maria Cristina T. Cangussú,[3] Antonio L. B. Pinheiro[2,3]

[1]Laser Center, IP&D, FCS, UNIVAP, Av. Shishima Ifume 2911, Urbanova, S. J. Campos, SP 12244-000, Brazil
[2]Universidade Camilo Castelo Branco Núcleo do Parque Tecnológico de São José dos Campos:Rod. Presidente Dutra Km 139—Eugênio de Melo, São José dos Campos, SP 12247-004, Brazil
[3]Center of Biophotonics, School of Dentistry, Federal University of Bahia, Av. Araújo Pinho, 62, Canela, Salvador, BA CEP 40140-110, Brazil

Abstract: Fractures have different etiology and treatment and may be associated or not to bone losses. Laser light has been shown to improve bone healing. We aimed to assess, through Raman spectroscopy, the level of CHA ($\sim$958 cm^{-1}) on complete fractures animals treated with IRF treated or not with Low Level Laser Therapy—LLLT and associated or not to BMPs and GBR. Complete tibial fractures were created on 15 animals that were divided into five groups. LLLT (Laser Unit, Kondortech, São Carlos, SP, Brazil, λ790 nm, 4 J/cm^2/point, 40 mW, φ $\sim$ 0.5 cm^2, 16 J/cm^2 session) started immediately after surgery and repeated at 48 h interval (2 weeks). Animal death occurred after 30 days. Raman spectroscopy was performed at the surface of the fracture. Our results showed significant differences between the groups IRF + BL /IRF_NBL ($p = 0.05$); between all experimental groups and untreated bone; bone/IRF + BL; IRF + BL + Bio + GBR; IRF + BL + LLLT; IRF + BL + Bio + GBR + LLLT; IRF_NBL ($p < 0.001$, all); IRF_NBL/IRF + BL + LLLT ($p = 0.03$); IRF_NBL/IRF + BL + Bio + GBR + LLLT ($p = 0.02$); IRF + BL/IRF + BL + LLLT ($p = 0.04$); IRF + BL/IRF + BL + Bio + GBR + LLLT ($p = 0.002$); IRF + BL + Bio + GBR/IRF + BL + Bio + GBR + LLLT ($p = 0.05$). It is concluded that the use of NIR LLLT associated to BMPs and GBR was effective in improving bone healing on fractured bones due to increased levels of CHA. © 2010 Wiley Periodicals, Inc. J Biomed Mater Res Part A: 94A: 1257–1263, 2010.

Key Words: biomaterials, bone healing, miniplates, laser therapy, traumatology

INTRODUCTION

Outside forces applied to bone has the potential to cause damage. A fracture is a loss of the integrity of the bone and its structure fails. Fractures occur when bone cannot withstand such forces. The healing of a fracture is an extremely interesting process in the human body. In optimal conditions, injured bone can be reconstituted without a scar almost identically to its original shape.

The healing of fractures occurs in three phases: inflammatory, reparative, and remodeling. Each one with specific cellular and biochemical phenomena and may be affected by both local and systemic factors. Local factors include the type of the trauma and bone loss, the type of bone affected, the degree of immobilization, and local pathologic conditions. The systemic factors include age, hormones, local stress, and electric currents. Natural processes of healing should be allowed to take their usual course and interference should be attempted only when there is demonstrable need or substantial advantages for the patient. Bone healing has been under extensive investigation for many years.

Fractures have been treated with immobilization, traction, amputation, and internal fixation throughout history. Immobilization by casting, bracing, or splinting a joint above and below the fracture was used for most long bone fractures. The treatment of fractures consists of the reduction and fixation of dislocated segments.[1]

The following principles are essential for a successful internal fracture fixation: anatomical reduction, stable internal fixation, preservation of the blood supply to bone fragments and soft tissues, and early and active pain-free mobilization. At present, most orthopedic surgeons carry out internal fixation of fractures based on these principles. However, these principles are now threatened by various advances on biomaterials and other modalities of treatment.

Internal fixation in the treatment of fractures should provide sufficient stability for fracture healing without excessive rigidity. The choice of internal fixation depends on the type of fracture, the condition of the soft tissues and bone, the size and position of the bone fragments, and the size of the bony defect.

Correspondence to: A. L. B. Pinheiro; e-mail: albp@ufba.br

The main goal of internal fixation is the achievement of prompt and, if possible, full function of the injured bone, with rapid rehabilitation of the patient. The majority of internal fixation devises are currently made of stainless steel. Occasionally, less strong, but biologically superior and more elastic, titanium implants are favored. Numerous devices are available for internal fixation. These devices can be roughly divided into a few major categories: wires; pins and screws; plates; and intramedullary nails or rods. Staples and clamps are also used occasionally for osteotomy or fracture fixation.

Traditional plate and screw constructs follow the tenets that include direct fracture exposure with anatomic reduction of fracture fragments and rigid internal fixation. The desired result of this intervention is the anatomic bone union. Complications using these techniques included delayed union, nonunion; refracture after device removal, and infection.[2]

Metal plates for internal fixation of fractures have been used for more than 100 years when Lane first introduced a metal plate for use in internal fixation. Lane's plate was eventually abandoned owing to problems with corrosion. Subsequently, Lambotte (1909) and then Sherman (1912) introduced their versions of the internal fracture fixation plate. Improvements in the metallurgical formulation of the plate increased their corrosion resistance; however, both designs were eventually abandoned as a result of their insufficient strength. Although initial shortcomings such as corrosion and insufficient strength have been overcome, more recent designs have not solved all problems.[2]

The majority of plates are made of stainless steel or titanium. With flexible fixation, the fracture fragments displace in relation to each other when the load is applied across the fracture site. Fracture fixation is considered flexible if it allows appreciable interfragmentary movement under functional load. The function of standard plate and screw constructs depends upon the stability requirements of a particular fracture. Plate–screw–bone constructs can act as load-sharing or load-bearing devices depending on fracture reduction and fragment interference.[2]

Conventional plating techniques are designed to provide absolute stability. When employed properly as compression plates or neutralization plates, conventional plates have the ability to resist axial, torsional, and bending loads. This is particularly true when no fracture gap exists and the plate is placed on the tension side of the fracture. Plate fixation may be used with or without cancellous bone grafting and, wherever possible should use compression. In general, it is agreed that compression has no specific beneficial effect on bone healing but is associated with improved stability of the fracture site.[2]

There are fractures whose handling is further complicated by the loss of bone. These losses may be related to several etiologies and require further efforts from the body to fully recover. Amongst the options available to minimize bone loses is the use of grafts. Despite grafts have been used to minimize the problems associated to bone loses, considerable limitations associated with the use of autografts and allografts have prompted an increased interest on the use of bone graft substitutes.[3,4]

The main types of commercially available bone graft substitutes are demineralized allograft bone matrix; ceramics and ceramic composites; composite graft of collagen and mineral; coralline hydroxyapatite; calcium phosphate cement; bioactive glass; and calcium sulfate.[4,6–10] The treatment of bone defects using biomaterials has been extensively studied elsewhere.[4–6] Since the pioneer work by Urist that demonstrated the heterotrophic formation of bone could be induced by devitalized demineralized bone matrix (DBM), a new possibility of treating bone defects has emerged.[6,7] The development and use of bone graft substitutes is a burgeoning field, and the review of all available products and their indications are beyond the scope of this article.

The healing of various types of bone defect with complete bone fill has been reported following the application of the Guided Bone Regeneration—GBR technique.[9] GBR is a technique used to prevent the migration of soft tissues, which has more pronounced proliferative activity, into the bone defect. GBR promotes bone formation by the use of a mechanical barrier such as membranes and these may be reabsorbable or nonreabsorbable and may also be associated or not to bone substitutes. The GBR is widely used for treating periodontal defects and other bone defects.[8]

Many techniques are used to improve the bone healing, recently, LLLT has been used for improving bone healing in several conditions such as in dental implants[11,12] and autologous bone graft,[5] and several types of bone defects.[4–7] Several studies have demonstrated that NIR Laser therapy is the most suitable for bone repair due to its higher penetration depth in the bone tissue when compared with visible laser light.[6] Although the use of LLLT on the bone healing has been growing steadily and several studies have demonstrated positive results on the healing of bone tissue, there are few reports on the association of LLLT and biomaterials.[6,7]

Raman scattering is a powerful light scattering technique used to diagnose the internal structure of molecules and crystals. Raman spectroscopy is the measurement of the wavelength and intensity of inelastically scattered light from molecules. The Raman scattered light occurs at wavelengths that are shifted from the incident light by the energies of molecular vibrations. The mechanism of Raman scattering is different from that of infrared absorption, and Raman and IR spectra provide complementary information. Typical applications are in structure determination, multicomponent qualitative analysis, and quantitative analysis.[10–14]

The Raman spectroscopy is an optical tool which could permit less invasive and nondestructive analysis of biological samples, allowing one to get precise information on biochemical composition.[10–14] It has been considered effective to assess tissues at the molecular level and has been used on several noninvasive diagnostic applications of biological samples such as cancers[13]; human coronary arteries[14,15]; blood analysis[16]; implants[17,18]; cell culture[19]; bone diseased[20]; bone healing[10–12,18]; to evaluate the microstructure of human cortical bone (osteon)[21] and biomaterials.[22] Raman spectroscopy has been accepted by many as a viable tool for the study of bone mineralization. The infrared

spectroscopy was preferred over Raman spectroscopy, due principally to the interference of Raman spectra with fluorescence from biological specimens.[19]

The Raman spectrum of bone shows prominent vibrational bands related to tissue composition. The Raman spectrum of bone shows prominent vibrational bands related to tissue composition. Some main Raman bands on tissues are at 862, 958, 1070, 1270, 1326, 1447, and 1668 cm^{-1}. The 1668 cm^{-1} band and the ones at 1270 and 1326 cm^{-1} are attributed to amide I and amide III stretching modes, the ones at 958 and 1070 cm^{-1} are attributed to phosphate and carbonate hydroxyapatite, respectively. The band at 862 cm^{-1} can be attributed to the vibration bands of C—C and C—C—H stretch of collagen and lipid. The band at 1447 cm^{-1} is attributed to the bending and stretching modes of CH groups of lipids and proteins.[11]

In a recent study,[12] Raman spectroscopy was used to investigate the effects of LLLT on the healing of dental implant of rabbits by monitoring the level of CHA in 15, 30, and 45 days after surgery. It was concluded that use of LLLT was effective in improving bone healing as a result of the increasing deposition of CHA, being this measured by Raman spectroscopy and compared with scanning electron microscopy.[11]

Our group has examined the same protocol used on this study using a different method of fracture fixation. We found that the use of LLLT associated to BMPs and GBR was effective in improving bone healing on fractured bones fixed with wire osteosynthesis as a result of the increasing deposition of CHA as measured by Raman spectroscopy.[10]

The aim of this study was to evaluate, through the analysis of Raman spectra intensity, the levels of calcium hydroxyapatite (CHA; 958 cm^{-1}; phosphate ν_1) on the repair of complete tibial fracture in rabbits treated by Internal Rigid Fixation (miniplates) associated or not to the use of LLLT (λ790 nm) and/or not to the use of BMPs and Guided Bone Regeneration.

MATERIALS AND METHODS

This study was approved by the Animal Ethics Committee of the Universidade do Vale do Paraíba. Fifteen healthy adult male New Zealand rabbits (average weight 2 kg) were kept under natural conditions of light, humidity, and temperature at the Animal House of the Instituto de Pesquisa e Desenvolvimento da Universidade do Vale do Paraíba during the experimental period. The animals were fed with standard laboratory pelted diet and had water ad libidum. The animals were kept in individual metallic gages; kept at day/night light cycle; and controlled temperature during the experimental period.

Under general anesthesia (0.2% Acepran®, 1 mg/kg (Univet SA, São Paulo, SP, Brazil, Butorfanol® 0.02 mL/kg, Fort Dodge Ltda, Campinas, SP, Brazil) and Zoletil® 50 mg, 15 mg/kg (VIRBAC S.A, Carro Cedex, France), the animals had the right leg shaved and a 4-cm long incision was performed at the right tibia with a No. 15 scalpel blade. Skin and subcutaneous tissues were dissected down to the periosteum, which was gently sectioned exposing the bone. One

TABLE I. Distribution of Each Animal on the Experimental Groups

Group	Treatment	Bone Loss	Biomaterial + Guided Bone Regeneration	LLLT
I	IRF[a]	Yes	No	No
II	IRF	Yes	Yes	No
III	IRF	Yes	No	Yes
IV	IRF	Yes	Yes	Yes
V	IRF_NBL[b]	No	No	No
VI	Bone	No	No	No

[a] Internal Rigid Fixation.
[b] Internal Rigid Fixation no bone loss.

tibial complete bone fracture was surgically produced (low speed drill, 1200 rpm, under refrigeration) in each animal. A 5 mm piece of bone was removed on all animals except on one group (IRF_NBL). The random distribution of the animals can be seen on Table I.

All groups had open fracture reduction and fixation with miniplates (Titanium). On the group IRF + Bone Loss, the fragments were fixed with the miniplates leaving a 5 mm gap; On groups IRF + Bone Loss + Biomaterial + GBR and IRF + Bone Loss + Biomaterial + GBR + LLLT, the defect was filled with lyophilized organic bovine bone (Gen-ox-org®) (Baumer S/A, Mogi Mirim, SP, Brazil 3), collagen (Gen-col®),[3] bone morphogenetic proteins (Gen-pro®),[3] and covered with decalcified cortical osseous membrane (Gen-derm®).[3] On groups IRF + Bone Loss + LLLT and IRF + Bone Loss + Biomaterial + GBR + LLLT (Diode Laser Unit, Kondortech, São Carlos, SP, Brazil, λ790 nm, 40 mW, $\phi \sim$ 0.5 cm^2) was transcutaneously applied in four points around the defects at 48-h intervals (4 J/cm^2, per point) being the first session carried out immediately after surgery and repeated at every 48 h during 15 days (16 J/cm^2 per session) and a total treatment dose of 112 J/cm^2. To standardize the location of irradiation, four tattoos were made on the skin using Nankin Ink around the fracture immediately after surgery to allow irradiation to be carried out at the same point. Doses used here based upon previous studies carried out by our group.[3] On group IRF_NBL, the fracture had no bone loss, was manually reduced and fixed with the miniplates. Normal bone acted as control (Bone).

All wounds were routinely sutured and the animals received a single dose of pentabiotico® (penicillin, streptomycin, 20.000UI, Fort Dodge Ltda, Campinas, SP, Brazil), immediately after surgery. The animals were humanely killed 30 days after the surgery with an overdose of general anesthetics.

The samples were longitudinally cut under refrigeration (Bueler®, Isomet TM1000; Markham, Ontario, Canada) and the specimens were stored in liquid nitrogen to minimize the growth of aerobics bacteria[12–14] and because the chemical fixation is not advisable due to fluorescence emissions from the fixative substances.[12–14]

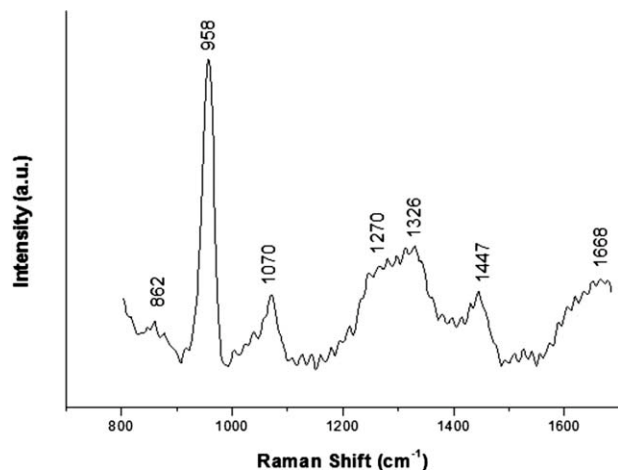Before Raman study, the samples were longitudinally cut and warmed gradually to room temperature and 100 mL of

FIGURE 1. Characteristic Raman spectrum of CHA (958 cm^{-1}, phosphate ν_1). Each peak corresponds to a specific bone component.

saline was added to the surface during spectroscopic measurements. For Raman measurements an $\lambda = 830$ nm Ti: Sapphire laser (Spectra Physics, model 3900S, Mountain View, CA, USA) pumped by Argon laser (Spectra Physics, model 2017S, Mountain View, CA, USA) provided near-infrared excitation. A spectrograph (Bruker Optics, model: 250 IS; Billerica, MA; USA) with spectral resolution of about 8 cm^{-1} dispersed the Raman scattered light from the sample and a liquid-nitrogen cooled deep depletion CCD (Princeton Instruments, model LN/CCD-1024-EHR1; Tucson, AZ; USA) detected the Raman spectra. The system was controlled by a microcomputer, which stored and processed the data.[9,11,12] The laser power used at the sample was of 80 mW, spectral acquisition time 100 s. Four points were measured in the transversal cut of the bone healing resulted in four readings of each specimen and 52 total spectra. All spectra were collected at the same day to avoid optical misalignments and changes in laser power. The mean value of the intensity of the peaks (958 cm^{-1}, phosphate ν_1) was determined by the average of the peaks on this region. This intensity is related to the concentration of CHA on the bone. The data were analyzed by the MatLab5.1® software (Newark, New Jersey, USA) software for calibration and background subtraction of the spectra. For calibration, the Raman spectrum of a solvent indene with known peaks was used[9,11,12] due to its intense bands in the region of (800–1800 cm^{-1}) our interest. It was also measured the indene spectrum each time the sample was changed to be sure that the laser and collection optics were optimized. To remove the "fluorescence background" from the original spectrum, a fifth order polynomial fitting was found to give better results facilitating the visualization of the peak of CHA ($\sim$958 cm^{-1}) found on the bone (Fig. 1). This routine can also remove any continuum, offset background noise, due to CCD readout and cooling. Statistical analysis was performed using Minitab 12.0® software (Minitab, Belo Horizonte, MG, Brazil). A baseline Raman spectrum of nontreated bone was also produced and acted as control.

RESULTS

The Raman spectrum of bone shows prominent vibrational bands related to tissue composition. Figure 1 shows the tissue main Raman bands at 862, 958, 1070, 1270, 1326, 1447, and 1668 cm^{-1}. The 1668 cm^{-1} band and the ones at 1270 and 1326 cm^{-1} are attributed to amide I and amide III stretching modes, the ones at 958 and 1070 cm^{-1} are attributed to phosphate and carbonate hydroxyapatite, respectively. The band at 862 cm^{-1} can be attributed to the vibration bands of C—C and C—C—H stretch of collagen and lipid. The band at 1447 cm^{-1} is attributed to the bending and stretching modes of CH groups of lipids and proteins.[19] Figure 2 shows the value of the mean intensity of each Raman shift of hydroxyapatite (CHA, 958 cm^{-1}) obtained from all readings of treated and untreated subjects. The intensity of the Raman shift is directly related to the concentration/incorporation of CHA by the bone. So, higher intensity represents higher concentration of CHA. The results of the mean readings and standard deviation can be seen on Table II.

The data was analyzed by Kolmogorov- Smirnov test (5%) and was found to be normally distributed ($p = 0.37$). The analysis of the results of the concentration of CHA showed significant differences between the experimental groups (Internal Rigid Fixation $+$ Bone Loss $-$ IRF and Internal Rigid Fixation $+$ No Bone Loss—IRF_NBL, $p = 0.05$, ANOVA) and between the experimental groups and untreated bone (Basal Bone $-$ Bone, $p < 0.001$, ANOVA). Paired T test showed significant differences between the untreated bone and the experimental groups IRF $+$ Bone Loss $-$ IRF ($p < 0.001$); Internal Rigid Fixation $+$ Bone Loss $+$ Biomaterial $+$ GBR $-$ IR $+$ B ($p < 0.001$); Internal Rigid Fixation $+$ Bone Loss $+$ LLLT $-$ IR $+$ L ($p < 0.001$); Internal Rigid Fixation $+$ Bone Loss $+$ Biomaterial $+$ GBR $+$ LLLT $-$ IR $+$ B $+$L ($p < 0.001$); Internal Rigid Fixation $+$

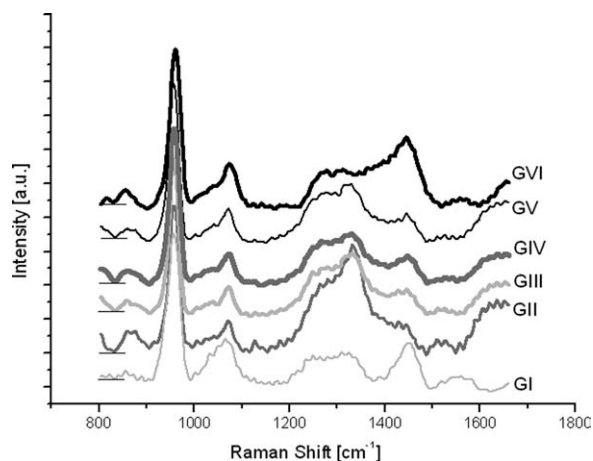**FIGURE 2.** Mean Raman shift of the surface concentration of CHA ($\sim$958 cm^{-1}) on the surface of tibial fractures treated with Internal Rigid Fixation. Each line corresponds to the mean spectrum found in each group. It is possible to see that untreated bone showed highest peak that was followed by the peaks on subjects treated with Internal Rigid Fixation $+$ Biomaterial $+$ Guided Bone Regeneration $+$ LLLT. The later was the treatment that got closer intensities of the peaks with untreated bone.

TABLE II. Mean Raman Shift ($\sim$958 cm^{-1}) of CHA on the Surface Treated with Internal Rigid Fixation

Group	Mean ± SD
Internal Rigid Fixation + Bone Loss (IRF)[a]	7438 ± 1393[b,c,d,e]
Internal Rigid Fixation + Bone Loss + Biomaterial + Guided Bone Regeneration (IRF + B)[f]	8132 ± 1946[c,e]
Internal Rigid Fixation + Bone Loss + Low Level Laser Therapy (IRF + L)[b]	8723 ± 1946[a,d,e]
Internal Rigid Fixation + Bone Loss + Biomaterial + Guided Bone Regeneration + Low Level Laser Therapy (IRF + L + B)[c]	9316 ± 711d[a,c,e,f]
Internal Rigid Fixation_No Bone Loss (IRF_NBL)[d]	7255 ± 2855[a,c,e,f]
Basal Bone[e]	11.974 ± 725[a,b,c,d,f]

[a,b,c,d,e,f] Groups that showed significant differences.

No Bone Loss—IRF_NBL − IRF_NBL ($p < 0.001$). Significant differences were also observed between groups Internal Rigid Fixation + No Bone Loss—IRF_NBL − IRF_NBL and Internal Rigid Fixation + Bone Loss + Bone Loss + LLLT − IRF + L ($p = 0.03$); Internal Rigid Fixation + No Bone Loss − IRF_NBL and Internal Rigid Fixation + Bone Loss + Biomaterial + GBR + LLLT − IRF + B + L ($p = 0.02$); Internal Rigid Fixation + Bone Loss − IRF and Internal Rigid Fixation + Bone Loss + LLLT − IRF + L ($p = 0.04$); IRF + Bone Loss − IRF and Internal Rigid Fixation + Bone Loss + Biomaterial + GBR + LLLT − IRF + B + L ($p = 0.002$); and between Internal Rigid Fixation + Bone Loss − IRF +B and Internal Rigid Fixation + Bone Loss + Biomaterial + GBR + LLLT − IRF + B + L ($p = 0.05$) (Fig. 3).

DISCUSSION

LLLT has been successfully used for improving bone healing in several conditions.[4] The effects of LLLT on bone are still controversial, as previous reports show different or conflicting results. It is possible that the effect of LLLT on bone regeneration depends not only on the total dose of irradiation but also on the irradiation time and the irradiation mode.[4] Many studies indicated that irradiated bone, mostly with IR wavelengths, shows increased osteoblastic proliferation, collagen deposition, and bone neoformation when compared with nonirradiated bone.[4] The irradiation protocol used in this study is similar to those used on previous reports.[4–7,10–12] Our group has shown, using different models, that association of bone grafts, bone morphogenetic proteins, and guided tissue regeneration does improve the healing of bone tissue.[4,11]

The healing of various types of bone defect with complete bone fill has been reported following the application of the Guided Bone Regeneration − GBR technique. GBR is a technique used to prevent the migration of soft tissues, which has more pronounced proliferative activity, into the bone defect. GBR promotes bone formation by the use of a mechanical barrier such as membranes and these may be reabsorbable or nonreabsorbable and may also be associated or not to bone substitutes. The GBR is widely used for treating periodontal defects and other bone defects. Our group has shown, using different models, that the association of bone grafts, BMPs and Guided Tissue Regeneration does improve the healing of bone tissue.[4–11]

Many studies indicated that irradiated bone, mostly with IR wavelengths, shows increased osteoblastic proliferation, collagen deposition, and bone neoformation when compared with nonirradiated bone.[4,10–12] The irradiation protocol used in this study is similar to those used on previous reports.[4,10–12]

Raman spectroscopy can be used to access the molecular constitution of a specific tissue and then classify it according to differences observed in the spectra.[15,22] Several studies found elsewhere on the literature have shown successful use of Raman spectroscopy as a diagnostic tool for healthy, diseased, or healing bones.[10–12,17–21]

The present investigation analyzed, by Raman spectroscopy, the intensity of the shift of the CHA ($\sim$958 cm^{-1}) on sites of complete tibial fractures in rabbits. The fractures were routinely treated by open reduction and Internal Rigid Fixation (miniplates). Because of the lack of report of the use of this model in the literature, the complete understanding of these initial findings is difficult. There are several aspects to consider on regards the technique used. Initially is important to consider that the repair of fractured bones is lengthy, when compared with other types of bony defects, and demands stability of the fragments in order not to develop nonunion. In our study, no such a case was found.

Our results showed that all treatment used on this study showed significant differences when compared with nontreated bone (Bone). It is important to note that the "conventional" internal rigid fixation technique was used on group IRF_NBL. On this group, there was no bone gap and the two fragments were plated together. On the other hand, all other experimental groups had a bone gap between them. It is clear that the standard internal rigid fixation
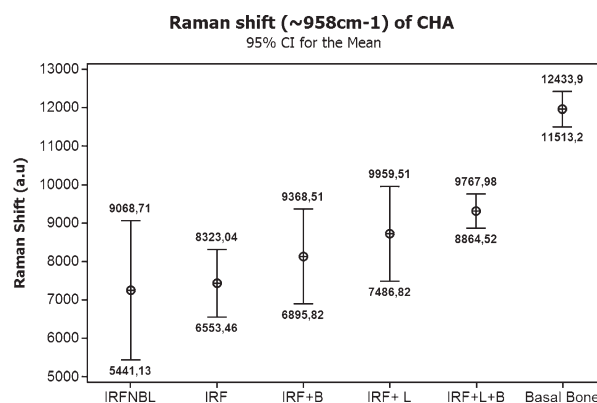

FIGURE 3. Averages of intensities of CHA ($\sim$958 cm^{-1}) on the surface of tibial fractures treated with Internal Rigid Fixation. The means of the peaks shows that untreated bone showed highest mean peaks of CHA and was followed by the peak observed on the group treated with Internal Rigid Fixation + Biomaterial + Guided Bone Regeneration + LLLT.

technique is not effective enough to restore the bone to its normal levels of CHA. It means that the bone on the fractured site is not fully matured and may not show the same mechanical properties of the normal bone. This has to be further investigated on studies using measurements of the strength of the fractured bone. Our results also showed significant differences between the different treatments themselves being the highest mean level of CHA found on IRF + Bone Loss + Biomaterial + GBR + L. This result shows that the association of the bone morphogenetic proteins, guided bone regeneration, and LLLT was more effective on bringing the level of CHA to the normality, even considering that there was a bone loss.[4–7,10–12]

We were also able to find significant differences between groups IRF_NBL and IRF + L; IRF_NBL and IRF + B + L; IRF and IRF + L; IRF and IRF + B + L; and between IRF + B and IRF + B + L. Most importantly we were unable to find differences on the level of CHA between IRF + B + L and Bone. This is indicative that the level of the deposition of CHA observed when we use the association of the bone morphogenetic proteins, guided bone regeneration, and LLLT was similar to the level of the untreated bone. This is complete agreement with reports on the literature.[4,11] This may also be indicative that the mechanical properties of this newly formed bone are similar to the one observed on normal bone.[12]

The present results are encouraging as fractures with bone loss in which the use of bone morphogenetic proteins, guided bone regeneration, and LLLT were used isolated or in association resulted in higher deposition of CHA than the observed when the internal rigid fixation was used alone with or without bone loss.

The results found on this study may be attributed to the fact that LLLT has the ability to stimulate cell proliferation, including fibroblasts; this cell has the capacity to secrete collagen. The use of the organic bone graft associated to LLLT resulted in better repair than that observed when the graft was used alone. Similar observations were reported previously.[4,7] This may represent an improved ability of more mature osteoblasts to secrete CHA on irradiated subjects, whereas in others groups, cell proliferation was still occurring. Deposition of CHA represents bone maturation. The results of this study indicate that LLLT associated to biomaterial grafts and guided bone regeneration, increased the concentration of CHA. Increased amount of CHA in bone is indicative of a more resistant bone.[4,10–12]

These results are very important clinically as we were able to show that we may have the restoration of normal levels of CHA on fractured sites within 30 days after trauma, even in cases in which bone losses occurred, using the association of the techniques we described. This would make possible the patient to go back to its routine life more rapidly.

CONCLUSIONS

It is concluded that the use of LLLT associated to bone morphogenetic proteins and guided bone regeneration was effective in improving bone healing on fractured bones treated with internal rigid fixation as a result of the increasing deposition of CHA measured by Raman spectroscopy.

REFERENCES

1. Erdogan Ö, Esen, E, Ustun Y, Kurkçu M, Akova T, Gonlusen G, Uysal H, Çevlik F. Effects of low-intensity pulsed ultrasound on healing of mandibular fractures: An experimental study in rabbits. J Oral Maxillofac Surg 2006;64:180–188.
2. Uhthoff HK, Poitras P, Backman DS. Internal plate fixation of fractures: Short history and recent developments. J Orthop Sci 2006; 11:118–126.
3. Fernández JR, Gallas M, Burguera M, Viãno JM. A three-dimensional numerical simulation of mandible fracture reduction with screwed miniplates. J Biomech 2003;36:329–337.
4. Pinheiro ALB, Gerbi MEMM. Photoengineering of bone repair processes. Photomed Laser Surg 2006;24:169–178.
5. Weber JB, Pinheiro ALB, Oliveira FA, Oliveira MG, Ramalho LMP. Laser therapy improves healing of bone defects submitted to autologous bone graft. Photomed Laser Surg 2006;24:38–44.
6. Pinheiro ALBP, Limeira Júnior FA, Gerbi MEMM, Ramalho LMP, Marzola C, Ponzi EAC. Effect of low level laser therapy on the repair of bone defects grafted with inorganic bovine bone. Braz Dent J 2003;14:177–181.
7. Gerbi MEMM, Pinheiro ALB, Marzola C, Limeira Júnior FA, Ramalho LMP, Ponzi EAC, Soares AO, Carvalho LCB, Lima HCAV, Gonçalves TO. Assessment of bone repair associated with the use of organic bovine bone and membrane irradiated at 830-nm. Photomed Laser Surg 2005;23:382–388.
8. Dimitriou R, Giannoudis PV. Discovery and development of BMPs. Injury 2005;365:528–533.
9. Ueyama Y, Koyama T, Ishikawa K, Mano T, Ogawa Y, Nagatsuka H, Suzuki K. Comparison of ready-made and self-setting alginate membranes used as a barrier membrane for guided bone regeneration. J Mater Sci Mater Med 2006;17:281–288.
10. Lopes CB, Pinheiro ALB, Sathaiah S, Silva NS, Salgado MC. Infrared laser photobiomodulation (830 nm) on bone tissue around dental implants: A Raman spectroscopy and scanning electronic microscopy study in rabbits. Photomed Laser Surg 2007;25: 96–101.
11. Lopes CB, Pacheco MTT, Silveira L Jr, Duarte J, Pinheiro ALB. The effect of the association of NIR laser therapy BMPs, and guided bone regeneration on tibial fractures treated with wire osteosynthesis: Raman spectroscopy study. J Photochem Photobiol B 2007;89:125–130.
12. Lopes CB, Pinheiro ALBP, Sathaiah S, Duarte J, Martins MC. Infrared laser light reduces loading time of dental implants: A Raman spectroscopy study. Photomed Laser Surg 2005;23:27–31.
13. Oliveira AP, Bitar RA, Silveira L Jr, Zangaro RA, Martin AA. Near-infrared Raman spectroscopy for oral carcinoma diagnosis. Photomed Laser Surg 2006;24:348–353.
14. Silveira-Júnior L, Sathaiah S, Zângaro RA, Pacheco MTT, Chavantes MC, Pasqualucci CA. Near infrared Raman spectroscopy of Human coronary arteries: Histopathological classification based on Mahalanobis distance. J Clin Laser Med Surg 2003;21: 203–208.
15. Nogueira GV, Silveira Júnior L, A Martin AA, Zângaro RA, Pacheco MTT, Chavantes MC, Pasqualucci CA. Raman spectroscopy study of atherosclerosis in human carotid artery. J Biomed Opt 2005;10:031117–1–031117–7.
16. Wood BR, Caspers P, Puppels GJ, Pandiancherri S, McNaughton D. Resonance Raman spectroscopy of red blood cells using near-infrared laser excitation. Anal Bioanal Chem 2007;387: 1691–1703.
17. Lopez-Heredia MA, Sohier J, Gaillard C, Quillard S, Dorget M, Layrolle P. Rapid prototyped porous titanium coated with calcium phosphate as a scaffold for bone tissue engineering. Biomaterials 2008;29:2608–2615.
18. Bozzini B, Carlino P, D'Urzo L, Pepe V, Mele C, Venturo F. An electrochemical impedance investigation of the behaviour of anodically oxidised titanium in human plasma and cognate fluids, relevant to dental applications. J Mater Sci Mater Med 2008;19: 3443–3453.

19. Morris MD, Stewart S, Tarnowski CP, Shea D, Franceschi R, Wang D, Ignelzi MA Jr, Wang W, Keller ET, Lin DL, Goldstein SA, Taboas JM. Early mineralization of normal and pathologic calvaria as revealed by Raman spectroscopy. SPIE Proc 2002;4614:28–39.

20. Carden A, Morris MD. Application of vibrational spectroscopy to the study of mineralized tissues (review). J Biomed Opt 2000;5: 259–268.

21. Schulmerich MV, Cole JH, Dooley KA, Morris MD, Kreider JM, Goldstein SA, Srinivasan S, Pogue BW. Noninvasive Raman tomographic imaging of canine bone tissue. J Biomed Opt 2008;13: 020506–1–020506–3.

22. Penel G, Delfosse C, Descamps M, Leroy G. Composition of bone and apatitic biomaterials as revealed by intravital Raman microspectroscopy. Bone 2005;36:893–901.